# Journal of Materials Chemistry A

Accepted Manuscript


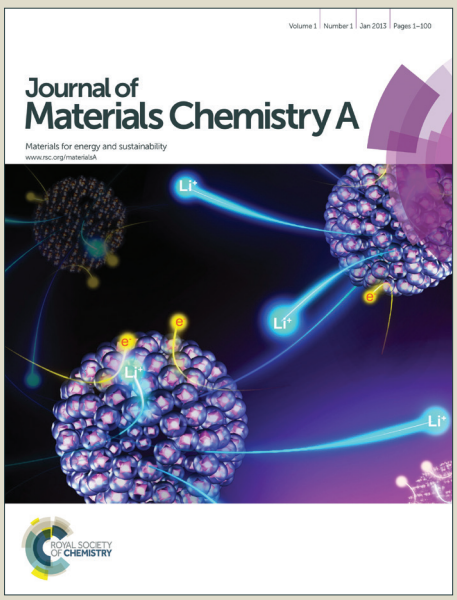



This is an *Accepted Manuscript*, which has been through the Royal Society of Chemistry peer review process and has been accepted for publication.

*Accepted Manuscripts* are published online shortly after acceptance, before technical editing, formatting and proof reading. Using this free service, authors can make their results available to the community, in citable form, before we publish the edited article. We will replace this *Accepted Manuscript* with the edited and formatted *Advance Article* as soon as it is available.

You can find more information about *Accepted Manuscripts* in the Information for Authors.

Please note that technical editing may introduce minor changes to the text and/or graphics, which may alter content. The journal's standard Terms & Conditions and the Ethical guidelines still apply. In no event shall the Royal Society of Chemistry be held responsible for any errors or omissions in this *Accepted Manuscript* or any consequences arising from the use of any information it contains.



ROYAL SOCIETY OF CHEMISTRY

www.rsc.org/materialsA

# Two (3,6)-connected porous metal-organic frameworks based on liner trinuclear $[Co_3(COO)_6]$ and paddlewheel dinuclear $[Cu_2(COO)_4]$ SBUs: gas adsorption, photocatalytic behaviour, and magnetic properties

Jun Zhao,[abc] Wen-Wen Dong,[a] Ya-Pan Wu,[a] Ye-Nan Wang,[a] Chao Wang,[a] Dong-Sheng Li,*[a] and Qi-Chun Zhang*[c,d]

[a]*College of Materials and Chemical Engineering, Hubei Provincial Collaborative Innovation Center for New Energy Microgrid, China Three Gorges University, Yichang, 443002, P. R. China. E-mail: lidongsheng1@126.com; Tel:+86 717 6397506*

[b]*State Key Laboratory of Structural Chemistry, Fujian Institute of Research on the Structure of Matter, Chinese Academy of Sciences, Fuzhou, 350002, P. R. China*

[c]*School of Materials Science and Engineering, Nanyang Technological University, Singapore 639798, Singapore. E-mail: qczhang@ntu.edu.sg; Tel: +65 67904705*

[d]*Division of Chemistry and Biological Chemistry, School of Physical and Mathematical Sciences, Nanyang Technological University, Singapore 637371 (Singapore)*

Journal of Materials Chemistry A Accepted Manuscript

**Abstract:**

Presented here are two novel (3,6)-connected porous metal-organic frameworks (MOFs) formulated as $[Co_3(BPT)_2(DMF)(bpp)]\cdot DMF$ (**1**) and $[(CH_3)_2NH_2][Cu(BPT)]\cdot DMF\cdot 2H_2O$ (**2**) ($H_3BPT$ = biphenyl-3,4′,5-tricarboxylic acid, bpp = 1,3-bis(4-pyridyl)propane). Compound **1** has a 3D neutral framework decorated with one-dimensional hydrophobic channels (the diameter 8.778(7) Å) while compound **2** is an anionic frameworks containing one-dimensional hydrophilic channels with the dimmer of 8.688(5) Å. Interestingly, compound **1** shows a promising visible-light-driven photocatalyst for the degradation of RhB while compound **2** exhibits high intake capacities for $CO_2$ (11.90 wt%) and $H_2$ (1.23 wt%), respectively. In addition, temperature-depended magnetic susceptibility measurements indicated that both **1** and **2** display dominated antiferromagnetic coupling among the adjacent Co(II) /Cu(II) centers.

Journal of Materials Chemistry A Accepted Manuscript

## Introduction

During the past two decades, the chemistry of porous materials has been revolutionized by the development of hybrid organic/inorganic porous materials known as metal-organic frameworks (MOFs).[1] These modularly synthesized and crystallographically ordered structures are composed of metal cluster nodes and rigid organic linkers. Because of their diverse and porous structures and ability to be post-synthetic modifications both in-pore and outer surface, MOFs have been employed as promising materials for usage in gas storage and separation, ion exchange, drug delivery, fuel reprocessing, sensing, environmental remediation, and catalysis.[2-6]

It has been widely believed that MOFs adsorb gas principally by physisorption, and one of the effective approaches to improve their affinity and gas selectivity is to build structures with smaller pore sizes, being slightly larger than the kinetic diameter of gas molecules, therefore the adsorbate can interact with more pore walls.[7] Furthermore, the pore surfaces with porous MOFs can be functionalized by the immobilization of specific sites, such as open metal sites, Lewis acidic and basic sites, to induce their stronger interactions with some gas molecules, thus reaching high storage and separation capacities and selectivity. In addition, recently, many efforts have been devoted to develop new photocatalytic materials based on MOFs, which is motivated largely by a demand for solving pollution problems in view of their potential applications in the green degradation of organic pollutants.[8] In contrast to the well-known semiconductor photocatalysts, the integration of semiconductivity, high crystallinity, and tunable porosity in these MOFs materials should offer large interfacial surface areas, shorter electron hole diffusion lengths to the internal interfaces, and multiple routes for band gap engineering through compositional and structural control.

As part of our investigations on the structural diversity, adsorptional and photocatalytic properties of metal aromatic polycarboxylic frameworks, some novel MOFs with gas adsorption and photocatalysis are reported in our previous work.[9] Herein, the trianionic form of biphenyl-3,4',5-tricarboxylic acid ($H_3$BPT) was selected as bridging ligands to build cluster complexes, which have been anticipated to possess outstanding photocatalytic and porous activities, and reasons are as follows: the tricarboxyl oxygen-donor linker with diversified chelating/bridging functions could have uncertain coordination capability to produce the porous structures,[10] and the coexistence of two benzene rings may make $H_3$BPT turn into a highly

Journal of Materials Chemistry A Accepted Manuscript

conjugated organic connector, which is likely to make the formed complexes carry potential optical properties.

In this contribution, solvothermal reactions of $H_3BPT$ and transition metal centers ($Co^{II}$/$Cu^{II}$) in the presence/absence of auxiliary ligand bpp have yielded $[Co_3(BPT)_2(DMF)(bpp)]\cdot DMF$ (**1**) and $[(CH_3)_2NH_2][Cu(BPT)]\cdot DMF\cdot 2H_2O$ (**2**). The X-ray diffraction analysis revealed that **1** and **2** exhibit neutral and anionic 3D frameworks decorated one-dimensional hydrophobic and hydrophilic channels, respectively. It is noted that compound **1** shows a high photocatalytic efficiency for the degradation of RhB, while, activated **2** demonstrates high uptake capacities for $CO_2$ (11.90 wt%) and $H_2$ (1.23 wt%).

## Experimental

### Materials and physical measurements

All chemicals were commercially available and used without further purification. FT-IR spectra (KBr pellets) were recorded on a Thermo Electron NEXUS 670 FTIR spectrometer. Elemental analyses were performed on a Perkin-Elmer 2400 Series II analyzer. Thermogravimetric (TG) curves were measured on a NETZSCH 449C thermal analyzer with a heating rate of 10 $^oC\ min^{-1}$ under air atmosphere. Powder X-ray diffraction (PXRD) were studied on a Rigaku Ultima IV diffractometer (Cu Kα radiation, λ = 1.5406 Å). The UV-vis spectra were obtained on a Shimadzu UV-2550 spectrometer. Variable-temperature magnetic susceptibility measurements were carried out on a Quantum Design MPMS-XL-7 SQUID magnetometer, and the diamagnetic corrections were evaluated by using Pascal's constants.[11] The simulated powder patterns were calculated using Mercury 2.0. The purity and homogeneity of bulk products were determined by the comparison of the simulated and experimental X-ray powder diffraction patterns.

### Preparation of $[Co_3(BPT)_2(DMF)(bpp)]\cdot DMF$ (1)

$CoCl_2\cdot 6H_2O$ (47.6 mg, 0.2 mmol), $H_3BPT$ (28.6 mg, 0.1 mmol), bpp (9.9 mg, 0.05 mmol), and 6 mL of DMF-$H_2O$ (2:1 in v/v) were placed in a Parr Teflon-lined stainless steel vessel (23 mL) and heated at 140 $^oC$ for 3 days. After the mixture was slowly cooled to room temperature, red crystals were obtained (yield: 82% based on Co). Elemental analysis: Calcd for $C_{55}H_{56}Co_3N_6O_{16}$: C, 53.54; H, 4.57; N, 6.81%; found: C, 53.80; H, 4.79; N, 7.03%. FT-IR (KBr pellets, $cm^{-1}$): 2928m, 2857w, 2358m, 2337m, 1680m, 1652s, 1614s, 1548s, 1438m, 1384s, 1106m, 1012w, 1007w, 773s, 719s,

Journal of Materials Chemistry A Accepted Manuscript

669m.

**Preparation of $[(CH_3)_2NH_2][Cu(BPT)]\cdot DMF\cdot 2H_2O$ (2)**

A mixture of $Cu(ClO_4)_2\cdot 6H_2O$ ( 74.1 mg, 0.2 mmol), $H_3BPT$ (28.6 mg, 0.1 mmol) was dissolved in 6 mL of DMF-$H_2O$ (2:1 in v/v) with a drop of 3 M $HNO_3$. The final mixture was placed in a Parr Teflon-lined stainless steel vessel (23 mL) and heated at 100 $^oC$ for 2 days. After the mixture was slowly cooled to room temperature, green crystals were obtained (yield: 70% based on Cu). **2** has a formula of $[(CH_3)_2NH_2][Cu(BPT)]\cdot DMF\cdot 2H_2O$, which was obtained based on single-crystal X-ray structural determination, elemental analysis and TGA. Elemental analysis. Calcd for $C_{20}H_{26}N_2CuO_9$: C, 47.85; H, 5.22; N, 5.58%; found: C, 41.62; H, 3.02; N, 13.37%. FT-IR (KBr pellets, $cm^{-1}$): 3452w, 3334w, 2955w, 2843w, 1654s, 1628s, 1577w, 1446w, 1399s, 1367s, 1301w, 1254 w, 1100w, 1081w, 1011w, 768s.

**X-ray crystallography study**

The diffraction data for compounds **1** and **2** were collected on a Rigaku XtaLAB mini diffractometer with graphite monochromated Mo *K*α radiation ($\lambda$ = 0.71073 Å). The collected data were reduced using the program *CrystalClear*[12] and an empirical absorption correction was applied. The structure was solved by direct methods and refined based on $F^2$ by the full matrix least-squares methods using SHELXTL.[13,14] All non-H atoms were refined anisotropically. The position of hydrogen atoms attached to carbon atoms were generated geometrically. For compound **1**: the atoms of DMF and bpp molecule are disordered over two positions with site occupancy factors of 0.18/0.82 for coordinated DMF molecule, 0.5/0.5 for free DMF molecule, 0.5/0.5 for bpp and the SADI restraint was used to make the corresponding bond distances approximately equal. In **2**, the $[(CH_3)_2NH_2]^+$ cations were generated during the synthesis by the hydrolysis of DMF,[15] and the charge-balancing $[(CH_3)_2NH_2]^+$ cations and all the guests in the pores are highly disordered and cannot be identified by single-crystal X-ray diffraction. The contribution of the disordered guests was subtracted from the reflection data by the PLATON/SQUEEZE method.[16] The resulting new files were used to further refine the structure. Crystallographic data and other pertinent information for **1** and **2** are summarized in Table 1, while the selected bond lengths and angles are listed in Table S1, ESI†.

Journal of Materials Chemistry A Accepted Manuscript

**Table 1** Crystal data and structure refinement details for **1** and **2**.

| | **1** | **2** |
|---|---|---|
| Empirical formula | $C_{55}H_{56}Co_3N_6O_{16}$ | $C_{15}H_7CuO_6$ |
| Formula weight | 1233.85 | 346.75 |
| Crystal system | $R\bar{3}$ | $R\bar{3}$ |
| space group | Trigonal | Trigonal |
| a /Å | 30.971(2) | 30.000(2) |
| b /Å | 30.971(2) | 30.000(2) |
| c /Å | 15.806(2) | 16.000(2) |
| $\alpha$/° | 90 | 90.000(2) |
| $\beta$ /° | 90 | 90.000(3) |
| $\gamma$ /° | 120 | 120.000(3) |
| $V$ /Å$^3$ | 13130.3(12) | 12470.8(10) |
| $Z$ | 9 | 18 |
| $F$(000) | 5733 | 3132 |
| $R$(int) | 0.0496 | 0.0916 |
| GOF | 1.048 | 1.076 |
| $R_1$[a)] [$I > 2\sigma(I)$] | 0.0787 | 0.0509 |
| w$R_2$[b)] [$I > 2\sigma(I)$] | 0.1720 | 0.1508 |
| $R_1$ (all data) | 0.0884 | 0.0619 |
| w$R_2$ (all data) | 0.1758 | 0.1594 |
| $\Delta\rho_{max, min}$ /e·Å$^{-3}$ | 1.085/-0.572 | 0.336/-0.613 |

a) $R_1 = \Sigma||F_0|| - |F_c|/\Sigma|F_0|$. b) $wR_2 = \{\Sigma[w(F_0^2 - F_c^2)^2]/\Sigma[w F_0^2]^2\}^{1/2}$

## Photocatalytic measurements

The evaluation of photocatalytic activities of the samples to degrade rhodamine B (RhB) was performed at ambient temperature (25 $^oC$). The procedure was as following: 0.050 g of sample was dispersed into 50 mL of RhB aqueous solution ($5\times10^{-5}$ mol $L^{-1}$), followed by the addition of five drops of hydrogen peroxide solution (30%). The suspension was shaken at a constant rate in the dark overnight (to establish an adsorption-desorption equilibrium of RhB on the sample surface). A 500 W xenon arc lamp was used as visible light source to irradiate the above solutions, which was continuously stirred during the degradation. At different time intervals, analytical samples were withdrawn from the reactor and the dispersed powders were removed by centrifugation. The resulted solutions were analyzed by UV/Vis spectroscopy.

## Sorption measurements

Journal of Materials Chemistry A Accepted Manuscript

The purity of all gases used for the gas sorption measurements is 99.999%. Low-pressure nitrogen ($N_2$), carbon dioxide ($CO_2$), methane ($CH_4$), ethylene ($C_2H_4$), ethane ($C_2H_6$) and hydrogen ($H_2$) sorption experiments (up to 1 bar) were performed on an ASAP 2020 surface area and pore size analyzer. The as-synthesized samples were treated by heating at 160 $^oC$ for 8 h in a quartz tube under vacuum to remove the solvent molecules prior to measurements. The sorption measurement was maintained at 77 K with liquid nitrogen and at 273 K with ice-water bath, respectively.

## Results and discussion

### Description of the crystal structures

**$[Co_3(BPT)_2(DMF)(bpp)]\cdot DMF$ (1).** Crystal structure analysis revealed that **1** crystallizes in the trigonal crystal system of the $R\bar{3}$ space group. The asymmetric unit of **1** includes one and a half independent Co(II) atoms, one $BPT^{3-}$ anion, half of bpp, and half of coordinated DMF molecule as well as half of free DMF molecule. Compound **1** consists of the centrosymmetric liner trinuclear cluster subunits $[Co_3(COO)_6]$ (Fig. 1a) linked by the branched organic spacer $BPT^{3-}$ *via* carboxylate bridging to other Co(II) centres. As shown in Fig.1a, Co1(II) atom adopts a distorted octahedral coordination geometry containing six oxygen atoms from six different $BPT^{3-}$ anions, while Co2(II) atom possesses a distorted octahedral mode coordinated with four carboxylate oxygen atoms, one nitrogen atom from bpp, and one oxygen atom from DMF molecule. The lengths of the Co–O bonds fall in the range of 1.978(4) -2.152(3) Å and the Co–N distance is about 2.140(4) Å. These data are similar to those reported for Co(II) complexes with $BPT^{3-}$ and N-donor ligands.[10b,17] Each $BPT^{3-}$ ligand coordinates to six Co(II) atoms through three different carboxylate groups adopting $\mu_2$-$\eta^1$:$\eta^1$, $\mu_2$-$\eta^1$:$\eta^1$ and $\mu_2$-$\eta^1$:$\eta^2$ coordination modes (I in Fig. S1, ESI). As a result, the liner trinuclear $[Co_3(COO)_6]$ clusters were linked by $BPT^{3-}$ and disordered bpp ligands into a 3D porous framework with a 1D hexagonal channel (Fig. 2d, S2†, S3†). It is remarkable that the 1D hexagonal channel as viewed along the *c*-axis has a diameter of about 8.778(7) Å. After removal of all disordered DMF molecules, the effective free void space of **1** is calculated by PLATON program as being 40.5% of the crystal volume (5313.5 Å out of the 13130.3 Å unit cell volume).

From a topological viewpoint, the $BPT^{3-}$ ligand can be viewed as a 3-connected node (Fig.

Journal of Materials Chemistry A Accepted Manuscript

1b), and bpp ligand can be defined as a linker and $[Co_3(COO)_6]$ cluster can be considered as a 6-connected node (Fig. 1c). Thus, the overall structure of **1** is a 3D (3,6)-connected **3,6T51** net with the point symbol of $\{4^2.6\}_2\{4^4.6^2.8^7.10^2\}$ (Fig. 1e). It was noted that similar trinuclear $[Co_3(COO)_6]$ units have been reported in other MOFs, however, they rarely presented as 6-connected nodes.[18]

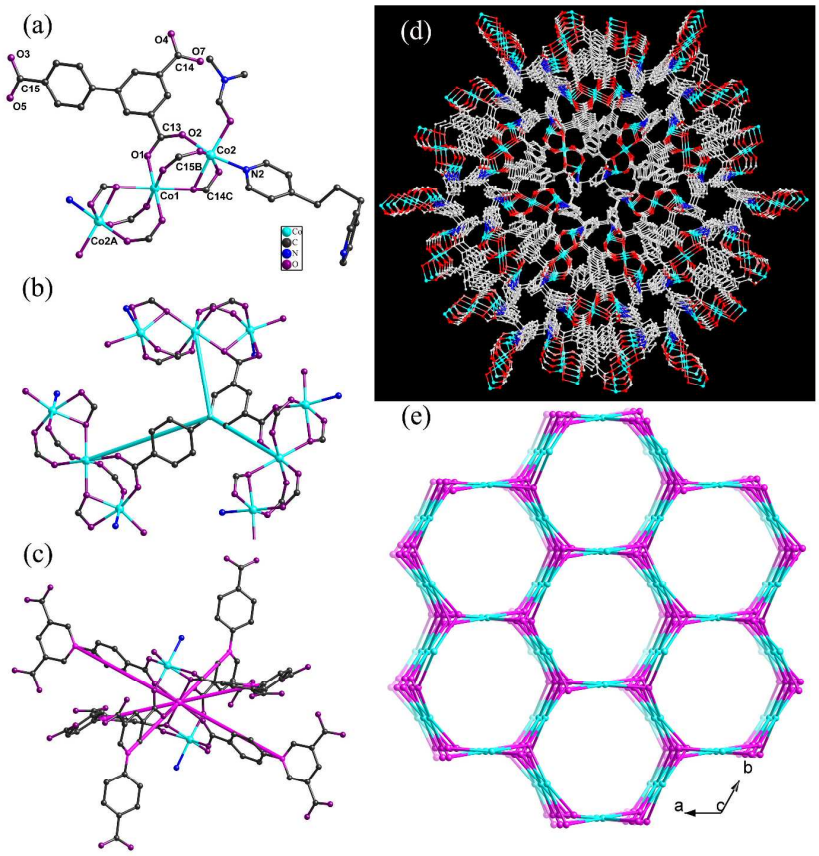


**Fig. 1** (a) The coordination environment of Co(II) atoms of **1** with hydrogen atoms omitted for clarity (A: -x+5/3, -y+1/3, -z+4/3; B: -y+4/3, x-y-1/3, z+2/3; C: x-y, x-1, 1-z); (b), (c) The schematic representation of 3-connected $BPT^{3-}$ ligand and 6-connected trinuclear $[Co_3(COO)_6]$ cluster; (d) View of the 3D framework with 1D hexagonal channel (the disordered DMF n molecules are omitted for clarity); (e) The topological view of the (3,6)-connected net with $\{4^2.6\}_2\{4^4.6^2.8^7.10^2\}$ topology.

**$[(CH_3)_2NH_2][Cu(BPT)]\cdot DMF\cdot 2H_2O$ (2).** Without the auxiliary ligand, $Cu(ClO_4)_2\cdot 6H_2O$ and $H_3BPT$ were used as the reactants and temperature was changed to 100 $^oC$, compound **2** was harvested. Compound **2** crystallizes in the trigonal crystal system of the $R\bar{3}$ space group. Each Cu(II) atom is coordinated by five carboxylate oxygen atoms from five different $BPT^{3-}$ ligands.

Journal of Materials Chemistry A Accepted Manuscript

Four carboxylate groups from different $BPT^{3-}$ groups cooridinate to a pair of Cu(II) atoms to generate the paddlewheel units (Cu···Cu distance of 2.722(6) Å), in which the axial positions are occupied by two carboxylate oxygen atoms from another two different $BPT^{3-}$ groups. Each $BPT^{3-}$ ligand coordinates to five Co(II) atoms through three carboxylate groups adopting $\mu_2$-$\eta^1$:$\eta^1$, $\mu_2$-$\eta^1$:$\eta^1$ and $\mu_1$-$\eta^1$:$\eta^0$ coordination modes, respectively (II in Fig. S1, ESI). Most surprisingly, the paddlewheel dinuclear $[Cu_2(COO)_4]$ secondary building units (SBUs) were bridged by the $BPT^{3-}$ ligands to form a 3D porous structure with a 1D hexagonal channel along the *c*-direction (Fig. 2d and Fig. S4†). It is noticeable that the inner surfaces of the hexagonal channels are mainly lined with the uncoordinated carboxylate oxygen atoms, suggesting a hydrophilic character with a diameter of 8.688(5) Å (based on inner carboxylate O···O separation). After removal of the guest molecules, the effective free void space of **2** is calculated by PLATON program as being 61.0% of the crystal volume (7612.9 Å out of the 12470.8 Å unit cell volume). Considering the paddlewheel $[Cu_2(COO)_4]$ units as a 6-connected node and the $BPT^{3-}$ group as a 3-connected node, the overall structure of **2** can be simplified as a (3,6)-connected **3,6T51** net, which is similar to **1** (Fig. 2b, c, e).

Although the $BPT^{3-}$ ligands in these two compounds exhibit different coordination configurations, both of them act as 3-connected nodes topologically, if trinuclear $[Co_3(COO)_6]$ clusters and dinuclear $[Cu_2(COO)_4]$ units are selected as 6-connected nodes. According to the topology definition of Wells, each of them features a (3,6)-connected topology with the point symbol of $\{4^2.6\}_2\{4^4.6^2.8^7.10^2\}$. Moreover, the carboxylate oxygen atoms, which lined in the inner hydrophilic channel surfaces in **2**, could provide a polar environment, where the hydrophobic pores with benzene rings of $BPT^{3-}$ ligands and bpp molecules are oriented inside the channel of **1**.

Journal of Materials Chemistry A Accepted Manuscript

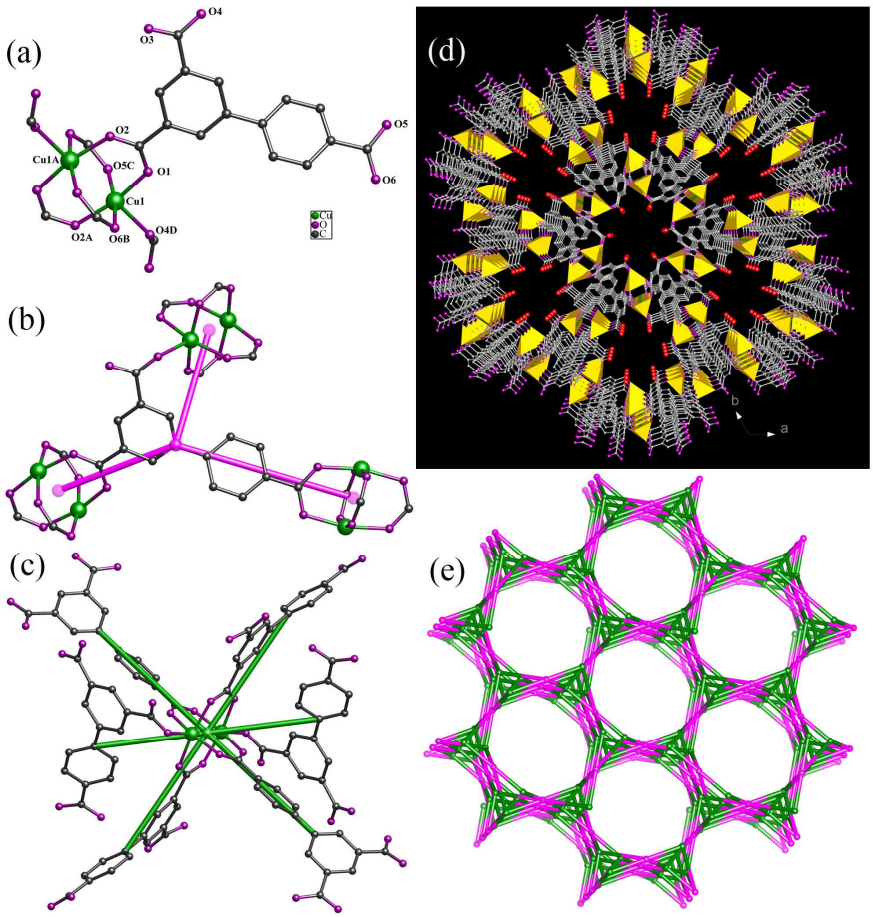


**Fig. 2** (a) The coordination environment of Cu(II) atoms of **2** with hydrogen atoms omitted for clarity (A: 1/3-x, 2/3-y, -1/3-z; B: 2/3+x-y, 1/3+x, 1/3-z; C: -1/3-x+y, 1/3-x; -2/3+z; D: 1/3-y, 2/3+x-y, -1/3+z); (b), (c) The schematic representation of 3-connected $BPT^{3-}$ ligand and 6-connected paddlewheel $[Cu_2(COO)_4]$ unit; (d) View of the 3D framework with 1D hexagonal channels; (e) The topological view of the (3,6)-connected net with $\{4^2.6\}_2\{4^4.6^2.8^7.10^2\}$ topology.

## PXRD and thermal stabilities of the compounds 1 and 2

The phase purities of compounds **1** and **2** were confirmed by PXRD measurements, and each PXRD pattern of the as-synthesized samples is consistent with the simulated ones (Fig. S5, ESI†). In order to investigate the mobility of the solvent molecules within MOFs, TGA was carried out for **1** and **2**, and the results are shown in Fig. S6, ESI†. In compound **1**, the continuous weight losses below 210 $^{o}$C corresponds to the loss of all DMF molecules (found 12.64 %, calcd.11.85 %), and the framework starts to decompose at approximately 320 $^{o}$C. Compound **2** shows a weight loss of 23.18% below 260 $^{o}$C, which is ascribed to the loss of free DMF and $H_2O$ molecules (cacld.

Journal of Materials Chemistry A Accepted Manuscript

21.74%). The Powder X-ray diffraction (PXRD) experiments under different temperatures were also performed to investigate the thermal stability of **2** upon the removal of all guest molecules according to the TG analysis. The PXRD patterns indicate that the framework starts to decompose at approximately 280 $^{o}$C and the XRD pattern after the removal of all guest molecules is obviously changed compared with that of the as-synthesized sample of **2** (Fig. S7, ESI†).

## Photocatalytic activities of 1

The band gap of compound **1** was investigated by UV-vis diffuse reflection measurement method at room temperature. The results give an $E_g$ (band gap energy) value of 2.10 eV (Fig. S8, ESI†), which is suitable for the photocatalytic measurement. In this research, an organic dye, rhodamine B (RhB), was used as a model pollutant in aqueous media to evaluate the photocatalytic effectiveness of **1** under xenon arc lamp illumination. The control experiments were carried out as following (Fig. 3): (a) with catalyst under visible light irradiation; (b) with $H_2O_2$ under visible light irradiation; and (c) with catalyst and $H_2O_2$ under visible light irradiation. The characteristic absorption (approximately 554 nm) of RhB was selected to monitor the adsorption and photocatalytic degradation process. The photocatalytic activity of **1** was gradually enhanced with time increasing from 0 to 120 min and nearly 90% of RhB was degraded (Fig. S9, ESI†). The proposed photocatalytic degradation mechanism was very similar to those of the previously reported.[8b,8c,19] The distinctly shortened degradation time compared with the control experiments underlines that catalyst **1** is active for the decomposition of RhB under visible-light irradiation. The kinetic data for the degradation of RhB can be well fitted by the apparent first-order rate equation and the rate constant under visible-light irradiation was found to be 1.15 $h^{-1}$. The PXRD pattern after photocatalytic experiment is almost the same as that of the as-prepared sample (Fig. S10, ESI†).

Journal of Materials Chemistry A Accepted Manuscript

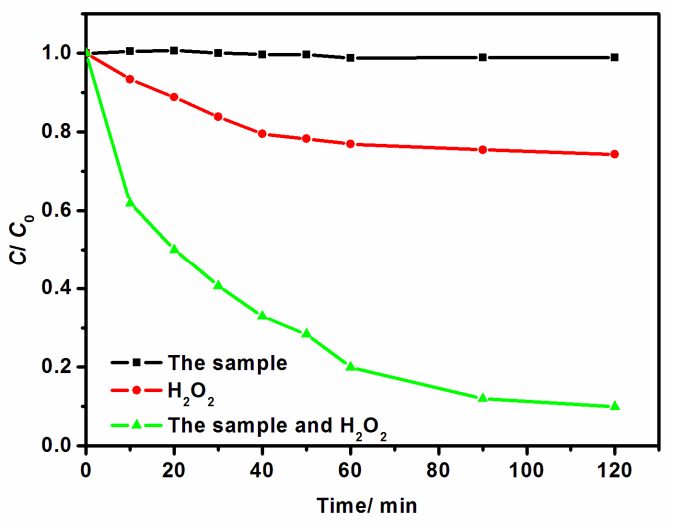


**Fig. 3** Photodecomposition of RhB dye in solution over different condition with visible light irradiation.

## Adsorption properties of compound 2.

Because of the framework of **1** was collapsed when the guest molecules were taken off in the vacuum condition, we didn't investigate the adsorption properties of the as-resulted sample after removing guest molecules from compound **1**. However, the framework of compound **2** is still remained after activating the crystals of compound **2** at 160 $^{o}$C for 8 h under high vacuum. The BET study (nitrogen sorption at 77 K) of compound **2** did show some interesting porosity. As shown in Fig. 4a, b, the experiment results display typical type I behavior, which is a characteristic of microporous materials. The maximum intake of $N_2$ at 1 bar for **2a** is 332 $cm^3g^{-1}$ (STP). The BET and Langmuir surface areas for **2a** are estimated to be 922.4 and 1286.2 $m^2g^{-1}$, respectively. A single data point at a relative pressure of 0.99 bar gives a pore volume of 0.514 $cm^3g^{-1}$ by the Horvath-Kawazoe equation.[20] The pore-size distributions from the analysis of the $N_2$ isotherm at 77K by using the Horvath-Kawazoe (HK) method suggest that the effective pore diameter for desolvated **2a** is 0.8701(5) nm, which is consistent with the value expected from the crystallographic data (*ca*. 0.8688(5) nm) (Fig. S11, ESI † ). Low-pressure hydrogen adsorption-desorption isotherms for **2** at 77 K is plotted in Fig. 4c and 4d, where no hysteresis is observed in the isotherms. Interestingly, a high amount of hydrogen (138.2 $cm^3$ $g^{-1}$, 6.17 mmol $g^{-1}$ or 1.23 wt%) for compound **2** at 77K is much higher than those for the reported mesoporous materials such as MCM-41(0.57 wt%) and Mirkin's amorphous infinite coordination polymer

Journal of Materials Chemistry A Accepted Manuscript

(0.57 wt%) under the same conditions.[21] On the other hand, the selective capture of $CO_2$ has been considered to be an effective way of controlling greenhouse gas emissions. It has been shown that MOFs and ZIFs can selectively intake large amounts of specific gases (e.g. carbon dioxide).[22] However, it still remains challenging to efficiently and selectively capture $CO_2$ from industrial emission streams (which invariably contain other gases such as $CH_4$, $N_2$ and so on), while, such a capability is very important for an efficient and economic reduction in $CO_2$ emissions. Thus, it is highly desirable to check if our materials have similar properties. In this research, the adsorption isotherms of $CO_2$, $CH_4$, $C_2H_4$, and $C_2H_6$ for **2a** were measured up to 1 bar at 273 K. As shown in Fig. 5, the uptake values are 60.56 $cm^3\ g^{-1}$ (2.70 mmol $g^{-1}$ or 11.90 wt%) for $CO_2$, 13.51 $cm^3\ g^{-1}$ (0.60 mmol $g^{-1}$ or 0.97 wt%) for $CH_4$, 32.07 $cm^3\ g^{-1}$ (1.43 mmol $g^{-1}$ or 4.0 wt%) for $C_2H_4$, and 31.18 $cm^3\ g^{-1}$ (1.39 mmol $g^{-1}$ or 4.17 wt%) for $C_2H_6$, respectively. The consequences of $CO_2$ and $CH_4$ indicated that **2a** has a relatively high selectivity for $CO_2/CH_4$ at 273 K. The $CO_2$ uptake is nearly 4.5 times larger than that of $CH_4$, and 2 times larger than that of $C_2H_4$ or $C_2H_6$ at 273 K. Such results could be explained through size-selective uptake because the bigger pore size has better match with the kinetic diameters of $CO_2$ molecules comparing to other gas molecules.[23] In addition, the big uptake of $CO_2$ can also be attributed to the electrostatic interactions with the uncoordinated carboxylate oxygens of the ligand. Our adsorption value is comparable to those of tris-*o*-phenylene-dioxycyclotriphosphazene containing 1D nanoporous channels (60.518 $cm^3\ g^{-1}$ at STP, 12 wt%, at 195K ).[24] In addition, the $CO_2$ uptake of 11.90 wt% at 273 K is comparable to that of the reported ZIFs such as ZIF-95/100 under the similar conditions.[25] Our results further prove that $H_3BPT$ is an excellent linker for the creation of the large area of porous MOFs due to its multiple coordination sites and rigid structure.[10] According to the searching results from Cambridge Structural Database (CSD version 5.35, Feb 2014), only thirteen MOFs constructed by $H_3BPT$ ligands exhibit $CO_2$ and/or $H_2$ adsorption so far.[26] In comparison with the reported compounds, the uptake of $CO_2$ and $H_2$ in compound **2a** is lower than the adsorption amount of derives from porhyrin-encapsulating **porph@MOM-10/ porph@MOM-11**, which represented the highest uptakes in the BPT-based MOFs, however, the uptake of **2a** is higher than those of **Cuporph@MOM-10-CdCu** and $Yb(BPT)(H_2O)\cdot(DMF)_{1.5}(H2O)_{1.25}$ under the similar conditions (Table S2, ESI†).

Journal of Materials Chemistry A Accepted Manuscript

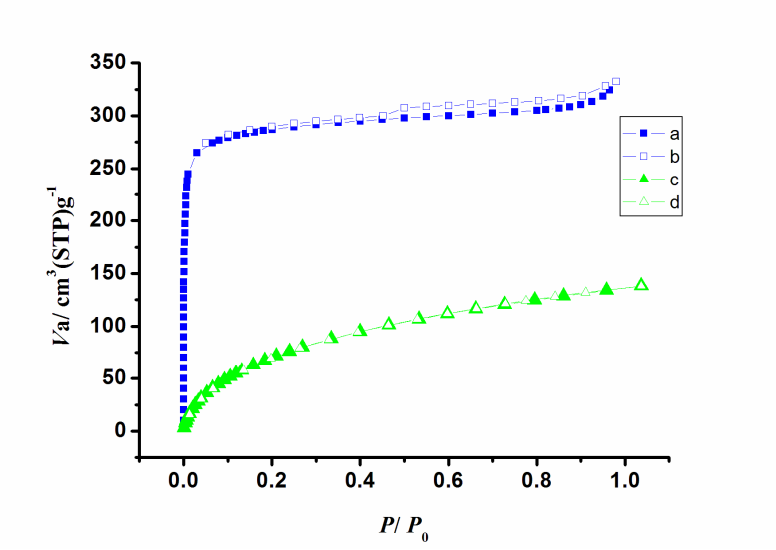


**Fig. 4** Gas sorption isotherms of **2a**: (a, b) $N_2$ adsorption and desorption at 77K; (c, d) $H_2$ adsorption and desorption at 77K.

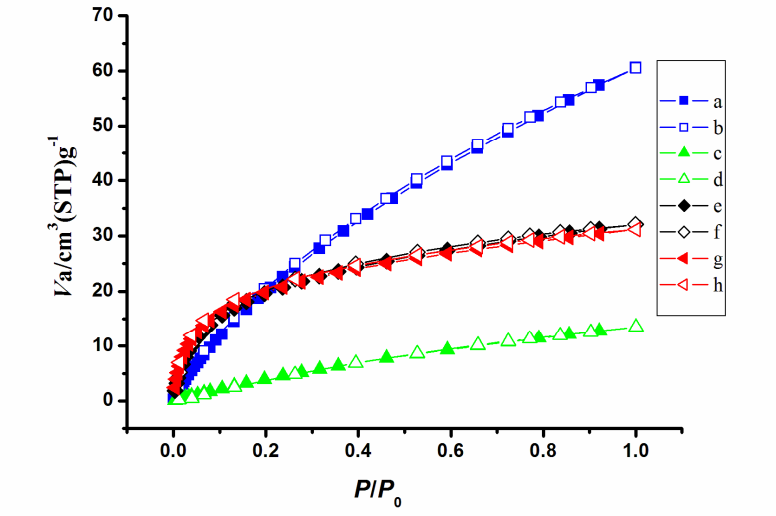


**Fig. 5** Gas sorption isotherms of **2a**: (a, b) $CO_2$ adsorption and desorption at 273K; (c, d) $CH_4$ adsorption and desorption at 273K; (e, f) $C_2H_4$ adsorption and desorption at 273K; (g, h) $C_2H_6$ adsorption and desorption at 273K.

## Magnetic properties

The temperature dependence of magnetic susceptibility of **1** and **2** in the form of $\chi_M$ and $\chi_M T$ versus $T$ were shown in Fig. 6. At room temperature, the $\chi_M T$ of **1** and **2** are 8.95 and 0.40 $cm^3$ K $mol^{-1}$, respectively. These values are obviously larger than those expected for three isolated Co(II) ions and one isolated Cu(II) ion (5.61 $cm^3$ K $mol^{-1}$ for three isolated Co(II) ions and 0.375 $cm^3$ K

Journal of Materials Chemistry A Accepted Manuscript

mol$^{-1}$ for one isolated Cu(II) ion), suggesting the strong orbital contribution.[27] For **1**, as the temperature decreases, the value of $\chi_M T$ slowly decreases and reaches a minimum value of 3.35 cm$^3$ K mol$^{-1}$ at 2K. For **2**, upon cooling, the $\chi_M T$ value decreases in the temperature range of 300−90 K with the strong antiferromagnetic coupling trend. In the temperature range of 90−35 K the $\chi_M T$ value decreases somewhat slowly and showed an approximate plateau with $\chi_M T$ value at about 0.23 cm$^3$ K mol$^{-1}$. This value is in the anticipated range for a spin doublet state. The above features are typical of isolated copper(II)-cluster species with antiferromagnetic coupling among metal ions.[28] Below 35 K, the $\chi_M T$ value decreases quickly down to 0.13 cm$^3$ K mol$^{-1}$ at 2K, indicating that the dinuclear units are not well isolated magnetically and that an antiferromagnetic interaction is operative among them. The data in the range of 130−300 K obeys the Curie-Weiss law with $C$ = 9.40, $\theta$ = -13.90 K for **1**, and $C$ = 0.63, $\theta$ = -168.86 K for **2**. The negative values of $\theta$ and the gradient of $\chi_M T$ *vs*. $T$ plots should be due to the dominated antiferromagnetic coupling between Co(II)/Cu(II) ions for **1** and **2**.

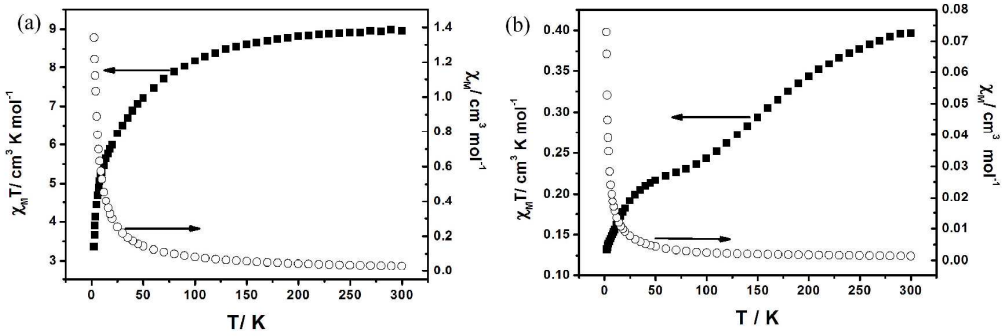


**Fig. 6** Temperature dependence of $\chi_M T$ and $\chi_M$ for **1** and **2**.

## Conclusions

In conclusion, we have successfully prepared two robust and porous Co(II)/Cu(II)- MOFs containing trinuclear [$Co_3(COO)_6$] and paddlewheel dinuclear [$Cu_2(COO)_4$] SBUs. Compounds **1** and **2** display a (3,6)-connected **3,6T51** net decorated with 1D hydrophobic or hydrophilic channels respectively. Compound **1** shows a high photocatalytic efficiency for the degradation of RhB, while, activated **2a** exhibits high uptake capacities for $CO_2$ (11.90 wt%) and $H_2$ (1.23 wt%), which suggests that compound **2** could have a great potential for $CO_2$ capturing and $H_2$ sorption. Future works will focus on the structures and properties of a series of coordination complexes constructed by $H_3$BPT ligand with other metal clusters.

**Electronic supplementary information (ESI) available:** Selected bond lengths and

Journal of Materials Chemistry A Accepted Manuscript

angles, PXRD, TG, UV/vis spectra, and additional figures. CCDC1033199 for **1**, CCDC1033200 for **2**. For ESI and crystallographic data in CIF or other electronic format see DOI:xxxxxx.

## Acknowledgements

This work was financially supported by the NSF of China (Nos. 21201109, 21373122, 21301106), the Project of Hubei Provincial Education Office (Nos. Q20131304, Q20141201) and the State Key Laboratory of Structural Chemistry, Fujian Institute of Research on the Structure of Matter, Chinese Academy of Sciences (20140015). Q.Z. acknowledges financial support from AcRF Tier 1 (RG 16/12) and Tier 2 (ARC 20/12 and ARC 2/13) from MOE, and the CREATE program (Nanomaterials for Energy and Water Management) from NRF, Singapore.

## Notes and references

1 (*a*) Metal-Organic Frameworks: Design and Application; L. R. MacGillivray, Ed, Wiley, Hoboken, 2010; (*b*) Special issue of *Chem. Soc. Rev.*, 2009, **38**, 1201-1508; (*c*) Special issue of *Chem. Rev.*, 2012, **112**, 673-1268.

2 (*a*) J. G. Duan, M. Higuchi, S. Horike, M. L. Foo, K. P. Rao, Y. Inubushi, T. Fukushima and S. Kitagawa, *Adv. Funct. Mater*., 2013, **23**, 3525; (*b*) B. S. Zheng, J. F. Bai, J. G. Duan, L. Wojtas and M. J. Zaworotko, *J. Am. Chem. Soc*., 2011, **133**, 748; (*c*) S. R. Batten and R. Robson, *Angew. Chem., Int. Ed*.1998, **37**, 1460; (*d*) R. Banerjee, A. Phan, B. Wang, C. Knobler, H. Furukawa, M. O'Keeffe and O.M. Yaghi, *Science*., 2008, **319**, 939; (*e*) S. L. Qiu, M. Xue and G. S. Zhu, *Chem. Soc. Rev*., 2014, **43**, 6116; (*f*) X. Zhao, M. Wong, C. Y. Mao, T. X. Trieu, J. Zhang, P. Y. Feng and X. H. Bu, *J. Am. Chem. Soc*., 2014, **136**, 12572.

3 (*a*) S. Horike, S. Shimomura and S. Kitagawa, *Nat. Chem*., 2009, **1**, 695; (*b*) J. S. Seo, D. Whang, H. Lee, S. I. Jun, J. Oh, Y. J. Jeon and K. Kim, *Nature*., 2000, **404**, 982; (*c*) C. E. Wilmer, M. Leaf, C.Y. Lee, O.K. Farha, B.G. Hauser, J. T. Hupp, R. Q. Snurr, *Nat. Chem*., 2012, **4**, 83; (*d*) J. R. Li, J. Sculley, H. C. Zhou, *Chem. Rev*., 2012, **112**, 869; (*e*) L. Zhang, H. B. Wu and X.W. Lou, *J. Am. Chem. Soc*., 2013, **135**, 10664; (*f*) J. K. Gao, J. W. Miao, P. Z. Li, W. Y. Teng, L. Yang, Y. L. Zhao, B. Liu and Q. C. Zhang, *Chem. Commun*., 2014, **50**, 3786; (*g*) J. K. Gao, L. L. Bai, Q. Zhang, Y. X. Li, G. Rakesh, J. M. Lee, Y. L. Yang and Q. C. Zhang, *Dalton Trans*., 2014**, 43** , 2559.

4 (*a*) M. Yoshizawa, J. K. Klosterman and M. Fujita, *Angew. Chem., Int. Ed*., 2009, **48**, 3418; (*b*)

Journal of Materials Chemistry A Accepted Manuscript

X. J. Kong, L. S. Long, Z. Zheng, R. B. Huang and L. S. Zheng, *Acc. Chem. Res*., 2010, **43**, 201; (*c*) E. B. Rusanov, V. V. Ponomarova, V. V. Komarchuk, H. Stoeckli-Evans, E. Fernandez-Ibanez, F. Stoeckli, J. Sieler and K. V. Domasevitch, *Angew. Chem., Int. Ed*., 2003, **42**, 2499; (*d*) H. S. Lu, L. L. Bai, W. W. Xiong, P. Z. Li, J. F. Ding, G. D. Zhang, T. Wu, Y. L. Zhao, J. M. Lee, Y. H. Yang, B. Y. Geng and Q. C. Zhang, *Inorg. Chem*., 2014, **53**, 8529.

5 (*a*) M. H. Zeng, M. X. Yao, H. Liang, W. X. Zhang and X. M. Chen, *Angew. Chem., Int. Ed*., 2007, **46**, 1832; (*b*) B. Liu, Y. P. Li, L. Hou, G. G. Yang, Y. Y. Wang and Q. Z. Shi, *J. Mater. Chem. A*., 2013, **1**, 6535; (*c*) D. Wu, G. Maurin, Q. Y. Yang, C. Serre, H. Jobic and C. L. Zhong, *J. Mater. Chem. A*., 2014, **2**, 1657; (*d*) J. K. Gao, K. Q. Ye, L. Yang, W. W. Xiong, L, Ye, Y. Wang and Q. C. Zhang, *Inorg. Chem*., 2014, **53**, 691; (*e*) G. P. Yang, L. Hou, L. F. Ma, Y. Y. Wang, *CrystEngComm*., 2013, **15**, 2561.

6 (*a*) L. Chen, F. L. Jiang, Z. Z. Lin, Y. F. Zhou, C. Y. Yue and M. C. Hong, *J. Am. Chem. Soc*., 2005, **127**, 8588; (*b*) D. S. Li, Y. P. Wu, J. Zhao, J. Zhang and J. Y. Lu, *Coord. Chem. Rev*., 2014, **261**, 1. (*c*) G. P. Yang, L. Hou, X. J. Luan, B. Wu, Y. Y. Wang, *Chem. Soc. Rev*., **2012**, **41**, 6992; (*d*) M. Du, C. P. Li, C. S. Liu and S. M. Fang, *Coord. Chem. Rev*., 2013, **257**, 1282.

7 X. M. Lin, T. T. Li, Y. W. Wang, L. Zhang and C. Y. Su*, Chem-Asian J*., 2012, **7**, 2796.

8 (*a*) C. C. Wang, J. R. Li, X. L. Lv, Y. Q. Zhang and G. S. Guo, *Energy Environ. Sci*., 2014, **7**, 2831; (*b*) L. L. Wen, L. Zhou, B. G. Zhang, X. G. Meng, H. Qu and D. F. Li, *J. Mater. Chem*., 2012, **22**, 22603; (c) T. Wen, D. X. Zhang, J. Liu, R. Lin and J. Zhang, *Chem. Commun*., 2013, 49*,* 5660.

9 (*a*) J. Zhao, D. S. Li, X. J. Ke, B. Liu, K. Zou and H. M. Hu, *Dalton Trans*., 2012, **41**, 2560; (*b*) D. S. Li, J. Zhao, Y. P. Wu, L. Bai and M. Du, *Inorg. Chem*., 2013, **52**, 8091; (*c*) D. S. Li, Y. P. Wu, P. Zhang, M. Du, J. Zhao, C. P. Li, Y. Y. Wang, *Cryst. Growth Des*., 2010, **10**, 2037; (*d*) T. Wen, D. X. Zhang, H. X. Zhang, H. B. Zhang, J. Zhang and D. S. Li, *Chem. Commun*., 2014, **50**, 8754; (*e*) J. Wang, J. H. Luo, J. Zhao, D. S. Li, G. H. Li, Q. S. Huo and Y. L. Liu, *Cryst. Growth Des*., 2014, **14**, 2375; (*f*) J. Zhao, D. S. Li, Z. Z. Hu, W. W. Dong, K. Zou and J. Y. Lu, *Inorg. Chem. Commun*., 2011, **14**, 771.

10 (*a*) W. W. He, S. L. Li, G. S. Yang, Y, Q. Lan, Z. M. Su and Q. Fu, *Chem. Commun*., 2012, **48**, 10001; (*b*) C. S. Lim, J. K. Schnobrich, A. G. Wong-Foy and A. J. Matzger, *Inorg. Chem*., 2010, **49**, 5271; (*c*) L. N. Li, S. Y. Wang, T. L. Chen, Z. H. Sun, J. H. Luo and M. C. Hong, *Cryst.*

Journal of Materials Chemistry A Accepted Manuscript

*Growth Des*., 2012, **12**, 4109; (*d*) D. Sun, L. L. Han, S. Yuan, Y. K. Deng, M. Z. Xu and D. F. Sun, *Cryst. Growth Des*., 2013, **13**, 377.

11 P. W. Selwood, Magnetochemistry, Interscience, New York, 1956.

12 Rigaku. CrystalClear version 2.0, Rigaku Corporation, Tokyo, Japan, 2009.

13 G. M. Sheldrick, SHELXS-97, Program for the Solution of Crystal Structures, University of Göttingen, Germany, 1997.

14 G. M. Sheldrick, SHELXL, Program for the Refinement of Crystal Structures, University of Göttingen, Germany, 1997.

15 A. C. Sudik, A. P. Côté, A. G. Wong-Foy, M. O'Keeffe, O. M. Yaghi, *Angew. Chem., Int. Ed*., 2006, 45, 2528

16 (*a*) P. Vandersluis and A. L. Spek, *Acta Crystallogr., Sect. A: Found. Crystllogr*., 1990, **46**, 94; (*b*) A. L. Spek, *J. Appl. Crystallogr*., 2003, **36**, 7.

17 C. C. Ji, J. Li, Y. Z. Li, Z. J. Guo and H. G. Zhen, *CrytEngComm*., 2011, **13**, 459.

18 (*a*) R. A. Reynolds III, W. R. Dunham and D. Coucouvanis, *Inorg. Chem*., 1998, **37**, 1232; (*b*) B. H. Ye, X. M. Chen, F. Xue, L. N. Ji and T. C. W. Mak*, Inorg. Chim. Acta*., 2000, **299**, 1.

19 F. Wang, Z. S. liu, H. Yang, Y. X. Tan, J. Zhang, *Angew. Chem., Int. Ed*., 2011, **50**, 450.

20 G. Horváth, K. Kawazoe, *J. Chem. Eng. Jpn*., 1983, **16**, 470.

21 (*a*) M. G. Nijkamp, J. Raaymakers, A. J. van Dillen and K. P. de Jong, *Appl. Phys. A: Mater. Sci. Process*., 2001, **72**, 619; (*b*) Y. M. Jeon, G. S. Armatas, J. Heo, M. G. Kanatzidis and C. A. Mirkin, *Adv. Mater*., 2008, **20**, 2105.

22 (*a*) H. Li, M. Eddaoudi, T. L. Groy and O. M. Yaghi, J. Am. Chem. Soc., 1998, **120**, 8571; (*b*) B. S. Zheng, R. R. Yun, J. F. Bai, Z. Y. Lu, L. T. Du and Y. Z. Li., *Inorg. Chem*., 2013, **52**, 2823.

23 K. Sumida, D. L. Rogow, J. A. Mason, T. M. McDonald, E. D. Bloch, Z. R. Herm, T. H. Bae and J. R. Long, *Chem. Rev*., 2012, **112**, 724.

24 (*a*) P. Sozzani, S. Bracco, A. Comotti, L. Ferretti and R. Simonutti, *Angew. Chem., Int. Ed*., 2005, **44**, 1816; (*b*) S. S. Chen, M. Chen, S. Takamizawa, M. S. Chen, Z. Su and W. Y. Sun, *Chem. Commun*., 2011, **47**, 752; (c) O. Shekhah, Y. Belmabkhout, Z. J. Chen, V. Guillerm, A. Cairns, K. Adil and M. Eddaoudi, *Nat. Commun*., 2014, **5**, 4228.

25 B. Wang, A. P. Côté, H. Furukawa, M. O'Keeffe and O. M. Yaghi, *Nature*., 2008, **453**, 207.

Journal of Materials Chemistry A Accepted Manuscript

26 (*a*) Z. Y. Guo, G. H. Li, L. Zhou, S. Q. Su, Y. Q. Lei, S. Dang and H. J. Zhang, *Inorg. Chem*., 2009, **48**, 8069; (*b*) Z. J. Zhang, W. Y. Gao, L. Wojtas, S. Q. Ma, M. Eddaoudi and M. J. Zaworotko, *Angew. Chem., Int. Ed*., 2012, **51**, 9330; (*c*) Z. Y. Guo, H. Xu, S. Q. Su, J. F. Cai, S. Dang, S. C. Xiang, G. D. Qian, H. J. Zhang, M. O'Keeffe and B. L. Chen, *Chem. Commun*., 2011, **47**, 5551; (*d*) A. G. Wong-Foy, O. Lebel and A. J. Matzger, *J. Am. Chem. Soc*., 2007, **129**, 15740; (*e*) Z. J. Zhang, L. P. Zhang, L. Wojtas, P. Nugent, M. Eddaoudi and M. J. Zaworotko, *J. Am. Chem. Soc*., 2012, **134**, 924; (*f*) Z. J. Zhang, L. Wojtas, M. Eddaoudi and M. J. Zaworotko, *J. Am. Chem. Soc*., 2013, **135**, 5982.

27 (*a*) S. Bhattacharya, A. Goswami, B. Gole, S. Ganguly, S. Bala, S. Sengupta, S. Khanra and R. Mondal, *Cryst. Growth Des*., 2014, **14**, 2853; (*b*) R. Patra, H. M. Titi and I. Goldberg, *CrytEngComm*., 2013, **15**, 7257.

28 (*a*) E. Q. Gao, Q. H. Zhao, J. K. Tang, D. Z. Liao, Z. H. Jiang and S. P. Yan, *J. Chem. Soc., Dalton Trans*., 2001, 1537; (*b*) A. B. Lago, J. Pasán, L. Cañadillas-Degada, Q. Fabelo, F. J. M. Casado, M. Julve, F. Lloret and C. Ruiz-Pérez. *New J. Chem*., 2011, **35**, 1817.

Journal of Materials Chemistry A Accepted Manuscript

## Graphical Abstract

**Two (3,6)-connected porous metal-organic frameworks based on liner trinuclear $[Co_3(COO)_6]$ and paddlewheel dinuclear $[Cu_2(COO)_4]$ SBUs: gas adsorption, photocatalytic behaviour, and magnetic properties**

Jun Zhao,[abc] Wen-Wen Dong,[a] Ya-Pan Wu,[a] Ye-Nan Wang,[a] Chao Wang,[a] Dong-Sheng Li,*[a] and Qi-Chun Zhang*[c,d]

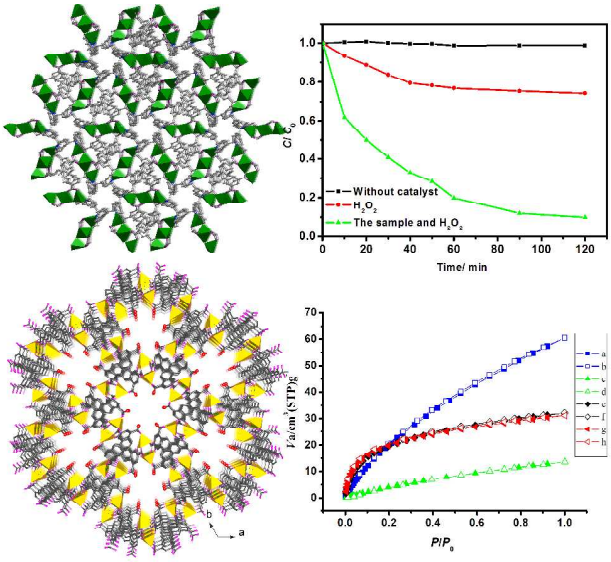


Journal of Materials Chemistry A Accepted Manuscript